

1 Effects of ocean acidification on pelagic carbon fluxes in a  
2 mesocosm experiment

3

4

5 Kristian Spilling<sup>1, 2</sup>, Kai G. Schulz<sup>3</sup>, Allanah J. Paul<sup>4</sup>, Tim Boxhammer<sup>4</sup>, Eric P. Achterberg<sup>4,</sup>  
6 <sup>5</sup>, Thomas Hornick<sup>6</sup>, Silke Lischka<sup>4</sup>, Annegret Stuhr<sup>4</sup>, Rafael Bermúdez<sup>4, 7</sup>, Jan Czerny<sup>4</sup>, Kate  
7 Crawford<sup>8</sup>, Corina P. D. Brussaard<sup>8, 9</sup>, Hans-Peter Grossart<sup>6, 10</sup>, Ulf Riebesell<sup>4</sup>

8 [1] {Marine Research Centre, Finnish Environment Institute, P.O. Box 140, 00251 Helsinki,  
9 Finland}

10 [2] {Tvärminne Zoological Station, University of Helsinki, J. A. Palménin tie 260, 10900  
11 Hanko, Finland}

12 [3] {Centre for Coastal Biogeochemistry, Southern Cross University, Military Road, East  
13 Lismore, NSW 2480, Australia}

14 [4] {GEOMAR Helmholtz Centre for Ocean Research Kiel, Düsternbrooker Weg 20, 24105  
15 Kiel, Germany}

16 [5] {National Oceanography Centre Southampton, European Way, University of  
17 Southampton, Southampton, SO14 3ZH, UK}

18 [7] {Facultad de Ingeniería Marítima, Ciencias Biológicas, Oceánicas y Recursos Naturales.  
19 ESPOL, Escuela Superior Politécnica del Litoral, Guayaquil, Ecuador}

20 [6] {Leibniz Institute of Freshwater Ecology and Inland Fisheries (IGB), Experimental  
21 Limnology, 16775 Stechlin, Germany}

22 [8] {NIOZ Royal Netherlands Institute for Sea Research, Department of Marine  
23 Microbiology and Biogeochemistry, and Utrecht University, P.O. Box 59, 1790 AB Den  
24 Burg, Texel, The Netherlands}

25 [9] {Department of Aquatic Microbiology, Institute for Biodiversity and Ecosystem  
26 Dynamics (IBED), University of Amsterdam, The Netherlands}

27 [10] {Potsdam University, Institute for Biochemistry and Biology, 14469 Potsdam,  
28 Germany}

29

30 Correspondence to: K. Spilling (kristian.spilling@environment.fi)

31 Running title: Modified pelagic carbon fluxes

32 Key words: Carbon fluxes, carbon budget, gross primary production, respiration, bacterial  
33 production, sinking carbon flux, CO<sub>2</sub> exchange with atmosphere

34 **Abstract**

35 About a quarter of anthropogenic CO<sub>2</sub> emissions are currently taken up by the oceans  
36 decreasing seawater pH. We performed a mesocosm experiment in the Baltic Sea in order to  
37 investigate the consequences of increasing CO<sub>2</sub> levels on pelagic carbon fluxes. A gradient of  
38 different CO<sub>2</sub> scenarios, ranging from ambient (~370 μatm) to high (~1200 μatm), were set  
39 up in mesocosm bags (~55 m<sup>3</sup>). We determined standing stocks and temporal changes of total  
40 particulate carbon (TPC), dissolved organic carbon (DOC), dissolved inorganic carbon (DIC)  
41 and particulate organic carbon (POC) of specific plankton groups. We also measured carbon  
42 flux via CO<sub>2</sub> exchange with the atmosphere and sedimentation (export); and biological rate  
43 measurements of primary production, bacterial production and total respiration. The  
44 experiment lasted for 44 days and was divided into three different phases (I: *t0-t16*; II: *t17-*  
45 *t30*; III: *t31-t43*). Pools of TPC, DOC and DIC were approximately 420, 7200 and 25200  
46 mmol C m<sup>-2</sup> at the start of the experiment, and the initial CO<sub>2</sub> additions increased the DIC  
47 pool by ~7% in the highest CO<sub>2</sub> treatment. Overall, there was a decrease in TPC and increase  
48 of DOC over the course of the experiment. The decrease in TPC was lower, and increase in  
49 DOC higher, in treatments with added CO<sub>2</sub>. During Phase I the estimated gross primary  
50 production (GPP) was ~100 mmol C fixed m<sup>-2</sup> d<sup>-1</sup>; from which 75-95% were respired, ~1%  
51 ended up in the TPC (including export) and 5-25% added to the DOC pool. During Phase II,  
52 the respiration loss increased to ~100% of GPP at the ambient CO<sub>2</sub> concentration, whereas  
53 respiration was lower (85-95% of GPP) in the highest CO<sub>2</sub> treatment. Bacterial production  
54 was ~30% lower, on average, at the highest CO<sub>2</sub> concentration compared with the controls  
55 during Phases II and III. This resulted in a higher accumulation DOC standing stock and  
56 lower reduction in TPC in the elevated CO<sub>2</sub> treatments at the end of Phase II extending  
57 throughout Phase III. The “extra” organic carbon at high CO<sub>2</sub> remained fixed in an increasing  
58 biomass of small-sized plankton and in the DOC pool, and did not transfer into large, sinking  
59 aggregates. Our results revealed a clear effect of increasing CO<sub>2</sub> on the carbon budget and  
60 mineralization, in particular under nutrient limited conditions. Lower carbon loss processes  
61 (respiration and bacterial remineralization) at elevated CO<sub>2</sub> levels resulted in higher TPC and  
62 DOC pools compared with the ambient CO<sub>2</sub> concentration. These results highlight the  
63 importance to address not only net changes in carbon standing stocks, but also carbon fluxes  
64 and budgets to better disentangle the effects of ocean acidification.

65

66 **1 Introduction**

67 Combustion of fossil fuels and change in land use, have caused increasing atmospheric  
68 concentrations of carbon dioxide (CO<sub>2</sub>). Ca. 25% of the anthropogenic CO<sub>2</sub> is absorbed by  
69 the oceans, thereby decreasing surface water pH, a process termed ocean acidification (Le  
70 Quéré et al., 2009). Ocean acidification and its alterations of aquatic ecosystems have  
71 received considerable attention during the past decade, but there are many open questions, in  
72 particular related to consequences for planktonic mediated carbon fluxes.

73 Some studies on ocean acidification have reported increased carbon fixation (Egge et al.,  
74 2009; Engel et al., 2013), bacterial production (Grossart et al., 2006) and bacterial  
75 degradation of polysaccharides (Piontek et al., 2010) at enhanced CO<sub>2</sub> levels, with potential  
76 consequences for carbon fluxes within pelagic ecosystems and export to the deep ocean, i.e.  
77 the biological carbon pump. Increasing carbon fixation in a high CO<sub>2</sub> environment can  
78 translate into an enhanced sequestration of carbon (Riebesell et al., 2007), but this depends on  
79 numerous environmental factors including phytoplankton community composition, aggregate  
80 formation and nutrient availability. For example, if the community shifts towards smaller cell  
81 sizes and/or enhanced cycling of organic matter carbon, export from the upper water layers  
82 may decrease (Czerny et al., 2013a).

83 The effect of ocean acidification has mostly been studied in marine ecosystems under high  
84 phytoplankton biomass. Brackish water has lower buffering capacity than ocean water and  
85 the pH fluctuates more. The limited number of studies of ocean acidification in brackish  
86 water and indications that ocean acidification effects are greatest under nutrient limitation  
87 (De Kluijver et al., 2010), motivated this mesocosm study in the Baltic Sea during low  
88 nutrient, summer months.

89 The Baltic Sea is functionally much like a large estuary, with a salinity gradient  
90 ranging from approximately 20 in the South-West to <3 in the Northernmost Bothnian Bay. It  
91 is an almost landlocked body of water with a large population in its vicinity (~80 million).  
92 Human activities (e.g. agriculture, shipping and fishing) cause a number of environmental  
93 problems such as eutrophication and pollution. As a coastal sea projected to change rapidly  
94 due to interaction of direct and indirect anthropogenic pressures, the Baltic Sea can be seen as  
95 a model ecosystem to study global change scenarios (Niiranen et al., 2013).

96 Most primary data from this experiment are published in several papers of this Special Issue  
97 (Riebesell et al., 2015). The aim of the present paper is to provide an overarching synthesis of

98 all information related to carbon standing stocks and fluxes. This enabled us to calculate  
99 carbon budgets in relation to different CO<sub>2</sub> levels.

100

101

## 102 **2 Materials and methods**

103

### 104 **2.1. Experimental set-up**

105 Six Kiel Off-Shore Mesocosms for future Ocean Simulations (KOSMOS; with a volume of  
106 ca. 55 m<sup>3</sup>) were moored at Storfjärden, on the south west coast of Finland (59° 51.5' N; 23°  
107 15.5' E) on 12 June 2012 (nine KOSMOS units were originally deployed but three were lost  
108 due to leaks). A more detailed description of the set-up can be found in Paul et al. (2015).  
109 The mesocosms extended from the surface down to 19 m depth and had a conical bottom end,  
110 which enabled quantitative collection of the settling material. Different CO<sub>2</sub> levels in the bags  
111 were achieved by adding filtered (50 µm), CO<sub>2</sub>-saturated seawater. The CO<sub>2</sub> enriched water  
112 was evenly distributed over the upper 17 m of the water columns and added in 4 consecutive  
113 time steps (*t0* – *t3*). Two controls and four treatments were used, and for the controls, filtered  
114 seawater (without additional CO<sub>2</sub> enrichment) was added. The CO<sub>2</sub> fugacity gradient after all  
115 additions ranged from ambient (average throughout the experiment: ~370 µatm *f*CO<sub>2</sub>) in the  
116 two control mesocosms (M1 and M5), up to ~1200 µatm *f*CO<sub>2</sub> in the highest treatment (M8).  
117 We used the average *f*CO<sub>2</sub> throughout this experiment (from *t1* – *t43*) to denote the different  
118 treatments: 365 (M1), 368 (M5), 497 (M7), 821 (M6), 1007 (M3) and 1231 (M8) µatm *f*CO<sub>2</sub>.  
119 On *t15*, additional CO<sub>2</sub>-saturated seawater was added to the upper 7 m in the same manner as  
120 the initial enrichment, to counteract outgassing of CO<sub>2</sub>.

121 We sampled the mesocosm every morning, but some variables were determined only every  
122 second day. Depth-integrated water samples (0 – 17 m) were taken by using integrating water  
123 samplers (IWS, HYDRO-BIOS, Kiel). The water was collected into plastic carboys (10 L)  
124 and taken to the laboratory for sub-sampling and subsequent determination of carbon stocks.

125

### 126 **2.2. Primary variables**

127 For more detailed descriptions of the primary variables and the different methods used during  
128 this CO<sub>2</sub> mesocosm campaign, we refer to other papers in this joint volume: i.e. total  
129 particulate carbon (TPC), dissolved organic carbon (DOC), and dissolved inorganic carbon  
130 (DIC) are described by Paul et al. (2015); micro and nanophytoplankton enumeration by  
131 Bermúdez et al. (2016); picophytoplankton, heterotrophic prokaryotes and viruses by  
132 Crawford et al. (2016); zooplankton community by Lischka et al. (2015); primary production  
133 and respiration by Spilling et al. (2016); bacterial production (BP) by Hornick et al. (2016);  
134 and sedimentation by Boxhammer et al. (2016); and Paul et al. (2015).

135 Briefly, samples for TPC (500 mL) were GF/F filtered and determined using an elemental  
136 analyser (EuroAE). DOC was measured using the high temperature combustion method  
137 (Shimadzu TOC –VCPN) following Badr et al. (2003). DIC was determined by infrared  
138 absorption (LI-COR LI-7000 on an AIRICA system). The DIC concentrations were  
139 converted from  $\mu\text{mol kg}^{-1}$  to  $\mu\text{mol L}^{-1}$  using the average seawater density of  $1.0038 \text{ kg L}^{-1}$   
140 throughout the experiment. Settling particles were quantitatively collected every other day  
141 from sediment traps at the bottom of the mesocosm units and the TPC determined from the  
142 processed samples (Boxhammer et al., 2016) as described above.

143 Mesozooplankton was collected by net hauls (100  $\mu\text{m}$  mesh size), fixed (ethanol) and  
144 counted in a stereomicroscope. Zooplankton carbon biomass (CB) was calculated using the  
145 displacement volume (DV) and the equation of Wiebe (1988):  $(\log DV + 1.429)/0.82 = \log$   
146 CB. Micro and nanoplankton (zoo- and phytoplankton) CB was determined from microscopic  
147 counts of fixed (acidic Lugol's iodine solution) samples, and the cellular bio-volumes were  
148 determined according to Olenina et al. (2006) and converted to POC by the equations  
149 provided by Menden-Deuer and Lessard (2000).

150 Picophytoplankton were counted using flow cytometry and converted to CB by size  
151 fractionation (Veldhuis and Kraay, 2004) and cellular carbon conversion factors ( $0.2 \text{ pg C}$   
152  $\mu\text{m}^{-3}$  (Waterbury et al., 1986). Prokaryotes and viruses were determined according to Marie et  
153 al. (1999) and Brussaard (2004), respectively. All heterotrophic prokaryotes, hereafter termed  
154 bacteria, and viruses were converted to CB assuming  $12.5 \text{ fg C cell}^{-1}$  (Heinänen and  
155 Kuparinen, 1991) and  $0.055 \text{ fg C virus}^{-1}$  (Steward et al., 2007), respectively.

156 The respiration rate was calculated from the difference between the O<sub>2</sub> concentration  
157 (measured with a Fibox 3, PreSens) before and after a 48 h incubation period in a dark,  
158 climate controlled room set to the average temperature observed in the mesocosms.

159 Bacterial protein production (BPP) was determined by  $^{14}\text{C}$ -leucine ( $^{14}\text{C}$ -Leu) incorporation  
160 (Simon and Azam, 1989) according to Grossart et al. (2006). The amount of incorporated  
161  $^{14}\text{C}$ -Leu was converted into BPP by using an intracellular isotope dilution factor of 2. A  
162 conversion factor of 0.86 was used to convert the produced protein into carbon (Simon and  
163 Azam, 1989).

164 Net primary production (NPP) was measured using radio-labeled  $\text{NaH}^{14}\text{CO}_3$  (Steeman-  
165 Nielsen, 1952). Samples were incubated for 24 h in duplicate, 8 ml vials moored on small  
166 incubation platforms at 2, 4, 6, 8 and 10 m depth next to the mesocosms. The areal primary  
167 production was calculated based on a simple linear model of the production measurements  
168 from the different depths (Spilling et al., 2016).

169

### 170 **2.3. Gas exchange**

171 In order to calculate the  $\text{CO}_2$  gas exchange with the atmosphere ( $\text{CO}_{2\text{flux}}$ ), we used  $\text{N}_2\text{O}$  as  
172 tracer gas, and this was added to mesocosm M5 and M8 (control and high  $\text{CO}_2$  treatment)  
173 according to Czerny et al. (2013b). The  $\text{N}_2\text{O}$  concentration was determined every second day  
174 using gas chromatography. Using the  $\text{N}_2\text{O}$  measurements, the fluxes across the water surface  
175 ( $F_{\text{N}_2\text{O}}$ ) was calculated according to:

$$176 \quad F_{\text{N}_2\text{O}} = I_{t_1} - I_{t_2} / (A * \Delta t) \quad (1)$$

177 where  $I_{t_1}$  and  $I_{t_2}$  is the bulk  $\text{N}_2\text{O}$  concentration at time:  $t_1$  and  $t_2$ ;  $A$  is the surface area and  $\Delta t$   
178 is the time difference between  $t_1$  and  $t_2$ .

179 The flux velocity was then calculated by:

$$180 \quad K_{\text{N}_2\text{O}} = F_{\text{N}_2\text{O}} / (C_{\text{N}_2\text{Ow}} - (C_{\text{N}_2\text{Oaw}})) \quad (2)$$

181 where  $C_{\text{N}_2\text{Ow}}$  is the bulk  $\text{N}_2\text{O}$  concentration in the water at a given time point, and  $C_{\text{N}_2\text{Oaw}}$  is  
182 the equilibrium concentration for  $\text{N}_2\text{O}$  (Weiss and Price, 1980).

183 The flux velocity for  $\text{CO}_2$  was calculated from the flux velocity of  $\text{N}_2\text{O}$  according to:

$$184 \quad k_{\text{CO}_2} = k_{\text{N}_2\text{O}} / (S_{\text{cCO}_2}/S_{\text{cN}_2\text{O}})^{0.5} \quad (3)$$

185 where  $S_{\text{cCO}_2}$  and  $S_{\text{cN}_2\text{O}}$  are the Schmidt numbers for  $\text{CO}_2$  and  $\text{N}_2\text{O}$ , respectively. The  $\text{CO}_2$  flux  
186 across the water surface was calculated according to:

187  $F_{\text{CO}_2} = k_{\text{CO}_2} (C_{\text{CO}_2\text{w}} - C_{\text{CO}_2\text{aw}})$  (4)

188 where  $C_{\text{CO}_2\text{w}}$  is the water concentration of  $\text{CO}_2$  and  $C_{\text{CO}_2\text{aw}}$  is the equilibrium concentration of  
189  $\text{CO}_2$ .  $\text{CO}_2$  is preferentially taken up by phytoplankton at the surface, where also the  
190 atmospheric exchange takes place. For this reason, we used the calculated  $\text{CO}_2$  concentration  
191 (based on the integrated  $\text{CO}_2$  concentration and pH in the surface) from the upper 5 m as the  
192 input for equation 5.

193 In contrast to  $\text{N}_2\text{O}$ , the  $\text{CO}_2$  flux can be chemically enhanced by hydration reactions of  $\text{CO}_2$   
194 with hydroxide ions and water molecules in the boundary layer (Wanninkhof and Knox,  
195 1996). Using the method outlined in Czerny et al. (2013b) we found an enhancement of up to  
196 12% on warm days and this was included into our flux calculations.

197

#### 198 **2.4. Data treatment**

199 The primary data generated in this study comprise of carbon standing stock measurements of  
200 TPC, DOC, DIC, as well as carbon estimates of meso- and microzooplankton, micro-, nano-  
201 and picophytoplankton, bacteria and viruses. Flux measurements of atmospheric  $\text{CO}_2$   
202 exchange and sedimentation of TPC, as well as the biological rates of net primary production  
203 ( $\text{NPP}_{14\text{C}}$ ), bacterial production (BP) and total respiration (TR) enabled us to make carbon  
204 budget.

205 Based on the primary variables (Chl *a* and temperature), the experiment where divided into  
206 three distinct phases: Phase I: *t0-t16*; Phase II: *t17-t30* and Phase III: *t31-t43*, where e.g.  
207 Chlorophyll *a* (Chl *a*) concentration was relatively high during Phase I, decreased during  
208 Phase II and remained low during Phase III (Paul et al. 2015). Measurements of pools and  
209 rates were average for the two first sampling points of each experimental phase ( $n = 2$ ) and  
210 where normalized to  $\text{m}^2$  knowing the total depth (17 m, excluding the sedimentation funnel)  
211 of the mesocosms. For fluxes and biological rates we used the average for the whole periods  
212 normalized to days ( $\text{day}^{-1}$ ). The rates of change ( $\Delta\text{TPC}$ ,  $\Delta\text{DOC}$  and  $\Delta\text{DIC}$ ) were the  
213 difference between the start and end of each phase. All error estimates were calculated as  
214 standard error (SE). The three different phases of the experiments were of different length  
215 with  $n = 16$ ,  $n = 14$  and  $n = 13$  for Phases I – III respectively. SE for estimated rates were  
216 calculated from the square root of the sum of variance for all the variables (Eq 5-10 below)

217 The primary papers mentioned above (section 2.2.) present detailed statistical analyses and  
218 we only refer to those here.

219 NPP was measured directly and we additionally estimated the net community production  
220 (NCP). This was done in two different ways from the organic (NCP<sub>o</sub>), dissolved plus  
221 particulate and inorganic (NCP<sub>i</sub>) fractions of carbon. NCP<sub>o</sub> was calculated from changes in  
222 the organic fraction plus the exported TPC (EXP<sub>TPC</sub>) according to:

$$223 \text{NCP}_o = \text{EXP}_{\text{TPC}} + \Delta\text{TPC} + \Delta\text{DOC} \quad (5)$$

224 Direct measurements using <sup>14</sup>C isotope incubations should in principal provide a higher value  
225 than summing up the difference in overall carbon balance (our NCP<sub>o</sub>), as the latter would  
226 incorporate total respiration and not only autotrophic respiration. NCP<sub>i</sub> was calculated  
227 through changes in the dissolved inorganic carbon pool, corrected for CO<sub>2</sub> gas exchange with  
228 the atmosphere (CO<sub>2</sub>flux) according to:

$$229 \text{NCP}_i = \text{CO}_{2\text{flux}} - \Delta\text{DIC} \quad (6)$$

230 In order to close the budget we estimated gross primary production (GPP) and DOC  
231 production (DOC<sub>prod</sub>). GPP is defined as the photosynthetically fixed carbon without any loss  
232 processes (i.e. NPP + autotrophic respiration). GPP can be estimated based on changes in  
233 organic (GPP<sub>o</sub>) or inorganic (GPP<sub>i</sub>) carbon pools, and we used these two different approaches  
234 providing a GPP range:

$$235 \text{GPP}_o = \text{NCP}_o + \text{TR} \quad (7)$$

$$236 \text{GPP}_i = \text{TR} + \text{CO}_{2\text{flux}} - \Delta\text{DIC} \quad (8)$$

237 During Phase III, TR was not measured and we estimated TR based on the ratios between  
238 NCP<sub>o</sub> and BP to TR during Phase II. The minimum production of DOC (DOC<sub>minp</sub>) in the  
239 system was calculated assuming bacterial carbon uptake was taken from the DOC pool  
240 according to:

$$241 \text{DOC}_{\text{minp}} = \Delta\text{DOC} + \text{BP} \quad (9)$$

242 However, this could underestimate DOC<sub>prod</sub> as a fraction of bacterial DOC uptake is respired.  
243 Without direct measurement of (heterotrophic prokaryote) bacterial respiration, (BR), we  
244 estimated BR from TR. The share of active bacteria contributing to bacterial production is  
245 typically in the range of 10-30% of the total bacterial community (Lignell et al., 2013). We



246 used the fraction of bacterial biomass (BB) of total biomass (TB) as the maximum limit of  
247 BR ( $BR \leq BB/TB$ ), and hence calculated max DOC production ( $DOC_{maxp}$ ) according to:

$$248 \quad DOC_{maxp} = \Delta DOC + BP + (BB * TR / TB) \quad (10)$$

249 We assumed that carbon synthesized by bacteria added to the TPC pool.

250 There are a number of uncertainties in these calculations, but this budgeting exercise provides  
251 an order-of-magnitude estimate of the flow of carbon within the system and enables  
252 comparison between the treatments. The average of the two controls (M1 and M5) and two  
253 highest CO<sub>2</sub> treatments (M3 and M8) were used to illustrate CO<sub>2</sub> effects.

254

### 255 **3. Results and discussion**

#### 256 **3.1 Change in plankton community, from large to small forms over time**

257 The overall size structure of the plankton community decreased over the course of the  
258 experiment. Fig 1 illustrates the carbon content in different plankton groups in the control  
259 mesocosms. During Phase I, the phytoplankton abundances increased at first in all treatments  
260 before starting to decrease at the end of Phase I (Paul et al., 2015). At the start of Phase II  
261 (t17), the phytoplankton biomass was higher than at the start of the experiment (~130 mmol  
262 C m<sup>-2</sup> in the controls) but decreased throughout Phase II and III. The fraction of  
263 picophytoplankton increased in all treatments, but some groups of picophytoplankton  
264 increased more in the high CO<sub>2</sub> treatments (Crawford et al., 2016).

265 Nitrogen was the limiting nutrient throughout the entire experiment (Paul et al., 2015), and  
266 primary producers are generally N-limited in the main sub-basins of the Baltic Sea  
267 (Tamminen and Andersen, 2007). The surface to volume ratio increases with decreasing cell  
268 size, and consequently small cells have higher nutrient affinity, and are better competitors for  
269 scarce nutrient sources than large cells (Reynolds, 2006). The prevailing N-limitation was  
270 likely the reason for the decreasing size structure of the phytoplankton community.

271 Micro and mesozooplankton standing stock was approximately half of the phytoplankton  
272 biomass initially, but decreased rapidly in the control treatments during Phase I (Fig 1). In the  
273 CO<sub>2</sub> enriched treatments the zooplankton biomass also decreased but not to the same extent  
274 as in the control treatments (Spilling et al., 2016). Overall, smaller species benefitted from the

275 extra CO<sub>2</sub> addition, but there was no significant negative effect of high CO<sub>2</sub> on the  
276 mesozooplankton community (Lischka et al., 2015).

277 Bacterial biomass was the main fraction of the plankton carbon throughout the experiment.  
278 The bacterial numbers largely followed the phytoplankton biomass with an initial increase  
279 then decrease during Phase I; increase during Phase II and slight decrease during Phase III  
280 (Crawfurd et al., 2016). The bacterial community was controlled by mineral nutrient  
281 limitation, bacterial grazing and viral lysis (Crawfurd et al., 2016), and bacterial growth is  
282 typically limited by N or a combination of N and C in the study area (Lignell et al., 2008;  
283 Lignell et al., 2013).

284 The bacterial carbon pool was higher than the measured TPC. Part of the bacteria must have  
285 passed the GFF filters (0.7 μm), and assuming pico- to mesoplankton was part of the TPC,  
286 >50% of the bacterial carbon was not contributing to the measured TPC. The conversion  
287 factor from cells to carbon is positively correlated to cell size, and there is consequently  
288 uncertainty related to the absolute carbon content of the bacterial pool (we used a constant  
289 conversion factor). However, bacteria is known to be the dominating carbon share in the  
290 Baltic Sea during the N-limited summer months (Lignell et al., 2013), and its relative  
291 dominance is in line with this.

292 Although there are some uncertainty in the carbon estimate (Jover et al. 2014), virus make up  
293 (due to their numerical dominance) a significant fraction of the pelagic carbon pool. Of the  
294 different plankton fractions the virioplankton have been the least studied, but their role in the  
295 pelagic ecosystem is ecologically important (Suttle, 2007; Brussaard et al., 2008; Mojica et  
296 al., 2016). Viral lysis rates were equivalent to the grazing rates for phytoplankton and for  
297 bacteria in the current study (Crawfurd et al., 2015). As mortality agents, viruses are key  
298 drivers of the regenerative microbial food web (Suttle, 2007; Brussaard et al., 2008). Overall,  
299 the structure of the plankton community reflected the nutrient status of the system. The  
300 increasing N-limitation favoring development of smaller cells, and increasing dependence of  
301 the primary producers on regenerated nutrients.

302

### 303 **3.2. The DIC pool and atmospheric exchange of CO<sub>2</sub>**

304 The DIC pool was the largest carbon pool: 3-4 fold higher than the DOC pool and roughly  
305 60-fold higher than the TPC pool (Tables 1-3). After the addition of CO<sub>2</sub>, the DIC pool was  
306 ~7% higher in the highest CO<sub>2</sub> treatment compared to the control mesocosms (Table 1). The

307 gas exchange with the atmosphere was the most apparent flux affected by CO<sub>2</sub> addition  
308 (Tables 1-3). Seawater in the mesocosms with added CO<sub>2</sub> were supersaturated, hence CO<sub>2</sub>  
309 outgassed throughout the experiment. The control mesocosms were initially undersaturated,  
310 hence ingassing occurred during Phases I and II (Fig 2). In the first part of Phase III, the  
311 control mesocosms reached equilibrium with the atmospheric *f*CO<sub>2</sub> (Fig. 2). The gas  
312 exchange had direct effects on the DIC concentration in the mesocosms (Fig. 3). From the  
313 measured gas exchange and change in DIC it is possible to calculate the biologically  
314 mediated carbon flux. In the mesocosms with ambient CO<sub>2</sub> concentration, the flux  
315 measurements indicated net heterotrophy throughout the experiment. The opposite pattern,  
316 net autotrophy, was indicated in the two mesocosms with the highest CO<sub>2</sub> addition (Fig 3; see  
317 also section 3.7.).

318

### 319 **3.3. The DOC pool, DOC production and remineralization**

320 The DOC pool increased throughout the experiment in all mesocosm bags, but more in the  
321 treatments with elevated CO<sub>2</sub> concentration. The initial DOC standing stock in all treatments  
322 was approximately 7200 mmol C m<sup>-2</sup>. At the end of the experiment, the DOC pool was ~2%  
323 higher in the two highest CO<sub>2</sub> treatments compared to the controls (Fig. 4), and there is  
324 statistical support for this difference between CO<sub>2</sub> treatments (Phase III, *p* = 0.05) (Paul et al.,  
325 2015). Interestingly, the data does not point to a substantially higher release of DOC at high  
326 CO<sub>2</sub> (Figs 4 and 5). The bacterial production was notably lower during Phases II and III in  
327 the high CO<sub>2</sub> treatments (Hornick et al., 2016), and of similar magnitude as the rate of change  
328 in DOC pool (Table 2 and 3), indicating reduced bacterial uptake and remineralization of  
329 DOC. The combined results suggest that the increase in the DOC pool at high CO<sub>2</sub> was  
330 related to reduced DOC loss (uptake by bacteria), rather than increased release of DOC by the  
331 plankton community, at elevated CO<sub>2</sub> concentration.

332 The Baltic Sea is affected by large inflow of freshwater containing high concentrations of  
333 refractory DOC such as humic substances, and the concentration in Gulf of Finland is  
334 typically 400-500 μmol C L<sup>-1</sup> (Hoikkala et al., 2015). The large pool of DOC and turn over  
335 times of ~200 days (Tables 1-3) is most likely a reflection of the relatively low fraction of  
336 labile DOC, but bacterial limitation of mineral nutrients can also increase turn over times  
337 (Thingstad et al., 1997).

338 The DOC pool has been demonstrated to aggregate into transparent exopolymeric particles  
339 (TEP) under certain circumstances, which can increase sedimentation at high CO<sub>2</sub> levels  
340 (Riebesell et al., 2007). We did not have any direct measurements of TEP, but any CO<sub>2</sub> effect  
341 on its formation is highly dependent on the plankton community and its physiological status  
342 (MacGilchrist et al., 2014). No observed effect of CO<sub>2</sub> treatment on carbon export suggests  
343 that we did not have a community where the TEP production was any different between the  
344 treatments used.

345

### 346 **3.4. The TPC pool and export of carbon**

347 There was a positive effect of elevated CO<sub>2</sub> on TPC relative to the controls. At the start of the  
348 experiment, the measured TPC concentration in the enclosed water columns was 400-500  
349 mmol C m<sup>-2</sup> (Table 1). The TPC pool decreased over time but less in the high CO<sub>2</sub> treatment  
350 and at the end of the experiment, the standing stock of TPC was ~6% higher (Phase III, p =  
351 0.01; Paul et al. (2015) in the high CO<sub>2</sub> treatment (Fig. 4).

352 The export of TPC was not dependent on the CO<sub>2</sub> concentration but varied temporally. The  
353 largest flux of TPC out of the mesocosms occurred during Phase I with ~6 mmol C m<sup>-2</sup> d<sup>-1</sup>. It  
354 decreased to ~3 mmol C m<sup>-2</sup> d<sup>-1</sup> during Phase II and was ~2 mmol C m<sup>-2</sup> d<sup>-1</sup> during Phase III  
355 (Table 1-3). The exported carbon as percent of average TPC standing stock similarly  
356 decreased from ~1.3% during Phase I to 0.3-0.5% during Phase III. The initial increase in the  
357 autotrophic biomass was the likely reason for relatively more of the carbon settling in the  
358 mesocosms in the beginning of the experiment whereas the decreasing carbon export was  
359 most likely caused by the shift towards a plankton community depending on recycled  
360 nitrogen. This reduced the overall suspended TPC and also the average plankton size in the  
361 community.

362

### 363 **3.5. Biological rates: respiration**

364 Total respiration (TR) was always lower in the CO<sub>2</sub> enriched treatments (Tables 1-3). The  
365 average TR was 83 mmol C m<sup>-2</sup> d<sup>-1</sup> during Phase I, and initially without any detectable  
366 treatment effect. The respiration rate started to be lower in the high CO<sub>2</sub> treatments,  
367 compared with the controls, in the beginning of Phase II. At the end of Phase II there was a  
368 significant difference (p = 0.02; Spilling et al., 2016) between the treatments (Table 2), and

369 40% lower respiration rate in the highest CO<sub>2</sub> treatment compared with the controls (Spilling  
370 et al., 2016).

371 Cytosol pH is close to neutral in most organisms, and reduced energetic cost for internal pH  
372 regulation (e.g. transport of H<sup>+</sup>) and at lower external pH levels could be one factor reducing  
373 respiration (Smith and Raven, 1979). Hopkinson et al. (2010) found indirect evidence for  
374 decreased respiration and also proposed that increased CO<sub>2</sub> concentration (i.e. decreased pH)  
375 reduced metabolic cost of remaining intracellular homeostasis. Mitochondrial respiration in  
376 plant foliage decreases in high CO<sub>2</sub> environments, possibly affected by respiratory enzymes  
377 or other metabolic processes (Amthor, 1991; Puhe and Ulrich, 2012). Most inorganic carbon  
378 in water is in the form of bicarbonate (HCO<sub>3</sub><sup>-</sup>) at relevant pH, and many aquatic autotrophs  
379 have developed carbon concentrating mechanisms (CCMs) (e.g. Singh et al., 2014) that could  
380 reduce the cost of growth (Raven, 1991). There are some studies that have pointed to savings  
381 of metabolic energy due to down-regulation of carbon concentrating mechanisms (Hopkinson  
382 et al., 2010) or overall photosynthetic apparatus (Sobrino et al., 2014) in phytoplankton at  
383 high CO<sub>2</sub> concentrations. Yet, other studies of the total plankton community have pointed at  
384 no effect or increased respiration at elevated CO<sub>2</sub> concentration (Li and Gao, 2012; Tanaka et  
385 al., 2013), and the metabolic changes behind reduced respiration, remains an open question.  
386 Membrane transport of H<sup>+</sup> is sensitive to changes in external pH, but the physiological  
387 impacts of increasing H<sup>+</sup> needs further study to better address effects of ocean acidification  
388 (Taylor et al., 2012). An important aspect is also to consider the microenvironment  
389 surrounding plankton; exchange of nutrients and gases takes place through the boundary  
390 layer, which might have very different pH properties than bulk water measurements (Flynn et  
391 al., 2012).

392

### 393 **3.6. Biological rates: bacterial production**

394 Bacterial production (BP) became lower in the high CO<sub>2</sub> treatment in the latter part of the  
395 experiment. During Phase I, BP ranged from 27 to 46 mmol C m<sup>-2</sup> d<sup>-1</sup> (Table 1). The  
396 difference in BP between treatments became apparent in Phases II and III of the experiment.  
397 The average BP was 18% and 24% higher in the controls compared to the highest CO<sub>2</sub>  
398 treatments during Phases II and III, respectively (Tables 2 and 3). Statistical support (p≤0.01)  
399 for a treatment effect during parts of the experiment is presented in Hornick et al. (2016).

400 The lower bacterial production accounted for ~40% of the reduced respiration during Phase  
401 II, and the reduced respiration described above could at least partly be explained by the lower  
402 bacterial activity. This raises an interesting question: what was the mechanism behind the  
403 reduced bacterial production/respiration in the high CO<sub>2</sub> treatment? There are examples of  
404 decreased bacterial production (Motegi et al 2013) and respiration (Teira et al., 2012) at  
405 elevated CO<sub>2</sub> concentration. However, most previous studies have reported no change  
406 (Allgaier et al., 2008) or a higher bacterial production at elevated CO<sub>2</sub> concentration  
407 (Grossart et al., 2006; Piontek et al., 2010; Endres et al., 2014). The latter was also supported  
408 by the recent study of Bunse et al. (2016), describing up-regulation of bacterial genes related  
409 to respiration, membrane transport and protein metabolism at elevated CO<sub>2</sub> concentration;  
410 albeit, this effect was not evident when inorganic nutrients had been added (high Chl *a*  
411 treatment).

412 In this study, the reason for the lower bacterial activity in the high CO<sub>2</sub> treatments could be  
413 due to either limitation and/or inhibition of bacterial growth or driven by difference in loss  
414 processes. Bacterial grazing and viral lysis was higher in the high CO<sub>2</sub> treatments during  
415 periods of the experiment (Crawford et al., 2016), and would at least partly be the reason for  
416 the reduced bacterial production at high CO<sub>2</sub> concentration.

417 N-limitation increased during the experiment (Paul et al., 2015), and mineral nutrient  
418 limitation of bacteria can lead to accumulation of DOC, i.e. reduced bacterial uptake  
419 (Thingstad et al., 1997), similar to our results. Bacterial N limitation is common in the area  
420 during summer (Lignell et al., 2013), however, this N-limitation was not apparently different  
421 in the controls (Paul et al., 2015), and CO<sub>2</sub> did not affect N-fixation (Paul et al., 2016). In a  
422 scenario where the competition for N is fierce, the balance between bacteria and similar sized  
423 picophytoplankton could be tilted in favor of phytoplankton if they gain an advantage by  
424 having easier access to carbon, i.e. CO<sub>2</sub> (Hornick et al., 2016). We have not found evidence  
425 in the literature that bacterial production will be suppressed in the observed pH range inside  
426 the mesocosms, varying from approximately pH 8.1 in the control to pH 7.6 in the highest  
427 *f*CO<sub>2</sub> treatment (Paul et al., 2015), although enzyme activity seems to be affected even by  
428 moderate pH changes. For example, some studies report on an increase in protein degrading  
429 enzyme leucine aminopeptidase activities at reduced pH (Grossart et al., 2006; Piontek et al.,  
430 2010; Endres et al., 2014), whereas others indicate a reduced activity of this enzyme  
431 (Yamada and Suzumura, 2010). A range of other factors affects this enzyme, for example the  
432 nitrogen source and salinity (Stepanauskas et al., 1999), and any potential interaction effects

433 with decreasing pH are not yet resolved. Any pH-induced changes in bacterial enzymatic  
434 activity could potentially affect bacterial production.

435

### 436 **3.7. Biological rates: primary production**

437 There was an effect of CO<sub>2</sub> concentration on the net community production based on the  
438 organic carbon fraction (NCP<sub>o</sub>). NCP<sub>o</sub> was higher during Phase I than during the rest of the  
439 experiments and during this initial phase without any apparent CO<sub>2</sub> effect. There was no  
440 consistent difference between CO<sub>2</sub> treatments for NPP<sub>14C</sub> ( $p > 0.1$ ), but NCP<sub>o</sub> increased with  
441 increasing CO<sub>2</sub> enrichment during Phase II (Phase II; linear regression  $p = 0.003$ ;  $R^2 = 0.91$ ).  
442 This was caused by the different development in the TPC and DOC pools. The pattern of  
443 gross primary production (GPP) was similar to NCP<sub>o</sub> during Phases I and II. During Phase III  
444 there were no respiration or NPP<sub>14C</sub> measurements and the estimated GPP is more uncertain.  
445 The NCP<sub>o</sub> and GPP indicated a smaller difference between treatments during Phase III  
446 compared with Phase II.

447 The measures of NPP<sub>14C</sub> and NCP<sub>o</sub> were of a similar magnitude (Tables 1-3). During Phase I,  
448 NPP<sub>14C</sub> < NCP<sub>o</sub> (Table 1), this relationship reversed for most treatments during Phase II, with  
449 the exception of the highest CO<sub>2</sub> levels (Table 2). The difference between NPP<sub>14C</sub> and NCP<sub>o</sub>  
450 suggests that observed reduction in respiration at elevated CO<sub>2</sub> could be mainly heterotrophic  
451 respiration. However, in terms of the NPP<sub>14C</sub> < NCP<sub>o</sub>, the uncertainty seems to be higher than  
452 the potential signal of heterotrophic respiration. This would also indicate that the NPP<sub>14C</sub>  
453 during Phase I have been underestimated, in particular for the control mesocosm M1. During  
454 Phase II, the NPP<sub>14C</sub> was higher than NCP<sub>o</sub>, except for the two highest CO<sub>2</sub> treatments, more  
455 in line with our assumption of NPP<sub>14C</sub> > NCP<sub>o</sub>. The systematic offset in NPP<sub>14C</sub> during Phase  
456 I could be due to changed parameterization during incubation in small volumes (8 mL,  
457 Spilling et al., 2016), for example increased loss due to grazing.

458 The results of the DIC pool and atmospheric exchange of CO<sub>2</sub> provides another way of  
459 estimating the net community production based on inorganic carbon (NCP<sub>i</sub>). There was some  
460 discrepancy between the NCP<sub>o</sub> and NCP<sub>i</sub> as the latter suggested net heterotrophy in the  
461 ambient CO<sub>2</sub> whereas the high CO<sub>2</sub> treatments were net autotrophic during all three phases of  
462 the experiment (Fig. 3). For the NCP<sub>o</sub> there was no indication of net heterotrophy at ambient  
463 CO<sub>2</sub> concentration. In terms of the absolute numbers, the NCP<sub>i</sub> estimate is probably more  
464 uncertain than NCP<sub>o</sub>. Calculating the CO<sub>2</sub> atmospheric exchange from the measurements of a

465 tracer gas involves several calculation steps (Eq 1-4), each adding uncertainty to the  
466 calculation. However, both estimations (NCP<sub>i</sub> and NCP<sub>o</sub>) indicate that increased CO<sub>2</sub>  
467 concentrations lead to higher overall community production, supporting our overall  
468 conclusion.

469

470

### 471 **3.8 Budget**

472 A carbon budget for the two control mesocosms and two highest CO<sub>2</sub> additions is presented  
473 in Fig. 5. During Phase I the estimated gross primary production (GPP) was ~100 mmol C  
474 fixed m<sup>-2</sup> d<sup>-1</sup>; from which 75-95% were respired, ~1% ended up in the TPC (including export)  
475 and 5-25% added to the DOC pool. The main difference between CO<sub>2</sub> treatments became  
476 apparent during Phase II when the NCP<sub>o</sub> was higher in the elevated CO<sub>2</sub> treatments. The  
477 respiration loss increased to ~100% of GPP at the ambient CO<sub>2</sub> concentration, whereas  
478 respiration was lower (85-95% of GPP) in the highest CO<sub>2</sub> treatment. Bacterial production  
479 was ~30% lower, on average, at the highest CO<sub>2</sub> concentration compared with the controls  
480 during Phase II. The share of NCP<sub>o</sub> of GPP ranged from 2% to 20% and the minimum flux to  
481 the DOC pool was 11% to 18% of TPC.

482 The overall budget was calculated by using the direct measurements of changes in standing  
483 stocks and fluxes of export, respiration and bacterial production rates. The most robust data  
484 are the direct measurements of carbon standing stocks and their development (e.g. ΔTPC).  
485 These are based on well-established analytical methods with relatively low standard error  
486 (SE) of the carbon pools. However, the dynamic nature of these pools made the relative SE  
487 for the rate of change much higher, reflecting that the rate of change varied considerably  
488 within the different phases.

489 The rate parameters, calculated based on conversion factors, have greater uncertainty,  
490 although their SEs were relatively low, caused by uncertainty in the conversion steps. For  
491 example, the respiratory quotient (RQ) was set to one, which is a good estimate for  
492 carbohydrate oxidation. For lipids and proteins the RQ is close to 0.7, but in a natural  
493 environment RQ is often >1 (Berggren et al., 2012), and is affected by physiological state e.g.  
494 nutrient limitation (Romero-Kutzner et al., 2015). Any temporal variability in the conversion  
495 factors would directly change the overall budget calculations, e.g. RQ affecting total  
496 respiration and gross primary production estimates. However, the budget provides an order-



497 of-magnitude estimate of the carbon flow within the system. Some of the parameters such as  
498 GPP were estimated using different approaches, providing a more robust comparison of the  
499 different treatments.

500 The primary effect of increasing CO<sub>2</sub> concentration was the higher standing stocks of TPC  
501 and DOC compared with ambient CO<sub>2</sub> concentration. The increasing DOC pool and  
502 relatively higher TPC pool were driven by reduced respiration and bacterial production at  
503 elevated CO<sub>2</sub> concentration. Decreasing respiration rate reduced the recycling of organic  
504 carbon back to the DIC pool. The lower respiration and bacterial production also indicates  
505 reduced remineralization of DOC. These two effects caused the higher TPC and DOC pools  
506 in the elevated CO<sub>2</sub> treatments. The results highlight the importance of looking beyond net  
507 changes in carbon standing stocks to understand how carbon fluxes are affected under  
508 increasing ocean acidification.

509

510

## 511 **Acknowledgements**

512 We would like to thank all of the staff at Tvärminne Zoological station, for great help during  
513 this experiment, and Michael Sswat for carrying out the TPC filtrations. We also gratefully  
514 acknowledge the captain and crew of R/V ALKOR (AL394 and AL397) for their work  
515 transporting, deploying and recovering the mesocosms. The collaborative mesocosm  
516 campaign was funded by BMBF projects BIOACID II (FKZ 03F06550) and SOPRAN Phase  
517 II (FKZ 03F0611). Additional financial support for this study came from Academy of Finland  
518 (KS - Decisions no: 259164 and 263862) and Walter and Andrée de Nottbeck Foundation  
519 (KS). TH and HPG were financially supported by SAW project TemBi of the Leibniz  
520 Foundation. CPDB was financially supported by the Darwin project, the Royal Netherlands  
521 Institute for Sea Research (NIOZ), and the EU project MESOAQUA (grant agreement  
522 number 228224).

523

524

525 **References**

- 526 Allgaier, M., Riebesell, U., Vogt, M., Thyrraug, R., and Grossart, H.-P.: Coupling of  
527 heterotrophic bacteria to phytoplankton bloom development at different pCO<sub>2</sub> levels: a  
528 mesocosm study, *Biogeosciences*, 5, 1007-1022, 2008.
- 529 Amthor, J.: Respiration in a future, higher-CO<sub>2</sub> world, *Plant, Cell & Environment*, 14, 13-20,  
530 1991.
- 531 Badr, E.-S. A., Achterberg, E. P., Tappin, A. D., Hill, S. J., and Braungardt, C. B.:  
532 Determination of dissolved organic nitrogen in natural waters using high temperature  
533 catalytic oxidation, *Trends in Analytical Chemistry*, 22, 819-827, 2003.
- 534 Berggren, M., Lapierre, J.-F., and del Giorgio, P. A.: Magnitude and regulation of  
535 bacterioplankton respiratory quotient across freshwater environmental gradients, *The*  
536 *ISME journal*, 6, 984-993, 2012.
- 537 Bermúdez, R., Winder, M., Stuhr, A., Almén, A.-K., Engström-Öst, J., and Riebesell, U.:  
538 Effect of ocean acidification on the structure and fatty acid composition of a natural  
539 plankton community in the Baltic Sea, *Biogeosciences Discuss*, 10.5194/bg-2015-669,  
540 2016.
- 541 Boxhammer, T., Bach, L. T., Czerny, J., and Riebesell, U.: Technical Note: Sampling and  
542 processing of mesocosm sediment trap material for quantitative biogeochemical  
543 analyses, *Biogeosciences Discuss*, 13, 2849-2858, 2016.
- 544 Brussaard, C. P.: Optimization of procedures for counting viruses by flow cytometry, *Appl*  
545 *Env Microbiol*, 70, 1506-1513, 2004.
- 546 Brussaard, C., Wilhelm, S. W., Thingstad, F., Weinbauer, M. G., Bratbak, G., Heldal, M.,  
547 Kimmance, S. A., Middelboe, M., Nagasaki, K., and Paul, J. H.: Global-scale processes  
548 with a nanoscale drive: the role of marine viruses, *Isme Journal*, 2, 575, 2008.
- 549 Bunse, C., Lundin, D., Karlsson, C. M., Vila-Costa, M., Palovaara, J., Akram, N., Svensson,  
550 L., Holmfeldt, K., González, J. M., and Calvo, E.: Response of marine bacterioplankton  
551 pH homeostasis gene expression to elevated CO<sub>2</sub>, *Nature Clim Change*, 2016.
- 552 Crawford, K. J., Riebesell, U., and Brussaard, C. P. D.: Shifts in the microbial community in  
553 the Baltic Sea with increasing CO<sub>2</sub> *Biogeosciences Discuss*, 10.5194/bg2015-606,  
554 2016.
- 555 Czerny, J., Schulz, K. G., Boxhammer, T., Bellerby, R., Büdenbender, J., Engel, A., Krug, S.  
556 A., Ludwig, A., Nachtigall, K., and Nondal, G.: Implications of elevated CO<sub>2</sub> on

557 pelagic carbon fluxes in an Arctic mesocosm study - an elemental mass balance  
558 approach, *Biogeosciences*, 10, 3109–3125, 10.5194/bg-10-3109-2013, 2013a.

559 Czerny, J., Schulz, K. G., Ludwig, A., and Riebesell, U.: A simple method for air/sea gas  
560 exchange measurement in mesocosms and its application in carbon budgeting,  
561 *Biogeosciences*, 10, 1379-1390, 2013b.

562 De Kluijver, A., Soetaert, K., Schulz, K. G., Riebesell, U., Bellerby, R., and Middelburg, J.:  
563 Phytoplankton-bacteria coupling under elevated CO<sub>2</sub> levels: a stable isotope labelling  
564 study, *Biogeosciences*, 7, 3783-3797, 2010.

565 Egge, J., Thingstad, J., Larsen, A., Engel, A., Wohlers, J., Bellerby, R., and Riebesell, U.:  
566 Primary production during nutrient-induced blooms at elevated CO<sub>2</sub> concentrations,  
567 *Biogeosciences*, 6, 877-885, 2009.

568 Endres, S., Galgani, L., Riebesell, U., Schulz, K.-G., and Engel, A.: Stimulated bacterial  
569 growth under elevated pCO<sub>2</sub>: results from an off-shore mesocosm study, *Plos One*, 9,  
570 e99228, 10.1371/journal.pone.0099228, 2014.

571 Engel, A., Borchard, C., Piontek, J., Schulz, K. G., Riebesell, U., and Bellerby, R.: CO<sub>2</sub>  
572 increases <sup>14</sup>C-primary production in an Arctic plankton community, *Biogeosciences*,  
573 10, 1291-1308, 2013.

574 Flynn, K. J., Blackford, J. C., Baird, M. E., Raven, J. A., Clark, D. R., Beardall, J., Brownlee,  
575 C., Fabian, H., and Wheeler, G. L.: Changes in pH at the exterior surface of plankton with  
576 ocean acidification, *Nature Clim Change*, 2, 510-513, 2012.

577 Grossart, H.-P., Allgaier, M., Passow, U., and Riebesell, U.: Testing the effect of CO<sub>2</sub>  
578 concentration on the dynamics of marine heterotrophic bacterioplankton, *Limnol*  
579 *Oceanogr*, 51, 1-11, 2006.

580 Heinänen, A., and Kuparinen, J.: Horizontal variation of bacterioplankton in the Baltic Sea,  
581 *Appl Env Microbiol*, 57, 3150-3155, 1991.

582 Hoikkala, L., Kortelainen, P., Soinne, H., and Kuosa, H.: Dissolved organic matter in the  
583 Baltic Sea, *J Mar Sys*, 142, 47-61, 2015.

584 Hopkinson, B. M., Xu, Y., Shi, D., McGinn, P. J., and Morel, F. M.: The effect of CO<sub>2</sub> on the  
585 photosynthetic physiology of phytoplankton in the Gulf of Alaska, *Limnol Oceanogr*,  
586 55, 2011-2024, 2010.

587 Hornick, T., Bach, L. T., Crawford, K. J., Spilling, K., Achterberg, E. P., Brussaard, C.,  
588 Riebesell, U., and Grossart, H.-P.: Ocean acidification indirectly alters trophic  
589 interaction of heterotrophic bacteria at low nutrient conditions, *Biogeosciences*  
590 *Discuss*, doi:10.5194/bg-2016-61, 2016.

591 Jover, L. F., Effler, T. C., Buchan, A., Wilhelm, S. W., and Weitz, J. S.: The elemental  
592 composition of virus particles: implications for marine biogeochemical cycles, *Nature*  
593 *Reviews Microbiology*, 12, 519-528, 2014.

594 Le Quéré, C., Raupach, M. R., Canadell, J. G., Marland, G., Bopp, L., Ciais, P., Conway, T.  
595 J., Doney, S. C., Feely, R. A., and Foster, P.: Trends in the sources and sinks of carbon  
596 dioxide, *Nature Geosci*, 2, 831-836, 2009.

597 Li, W., and Gao, K.: A marine secondary producer respire and feeds more in a high CO<sub>2</sub>  
598 ocean, *Marine pollution bulletin*, 64, 699-703, 2012.

599 Lignell, R., Hoikkala, L., and Lahtinen, T.: Effects of inorganic nutrients, glucose and solar  
600 radiation on bacterial growth and exploitation of dissolved organic carbon and nitrogen  
601 in the northern Baltic Sea, *Aquat Microb Ecol*, 51, 209-221, 2008.

602 Lignell, R., Haario, H., Laine, M., and Thingstad, T. F.: Getting the “right” parameter values  
603 for models of the pelagic microbial food web, *Limnol Oceanogr*, 58, 301-313, 2013.

604 Lischka, S., Bach, L. T., Schulz, K.-G., and Riebesell, U.: Micro- and mesozooplankton  
605 community response to increasing levels of *f*CO<sub>2</sub> in the Baltic Sea: insights from a  
606 large-scale mesocosm experiment, *Biogeosciences Discuss*, 10.5194/bgd-12-20025-  
607 2015, 2015.

608 MacGilchrist, G., Shi, T., Tyrrell, T., Richier, S., Moore, C., Dumousseaud, C., and  
609 Achterberg, E. P.: Effect of enhanced pCO<sub>2</sub> levels on the production of dissolved  
610 organic carbon and transparent exopolymer particles in short-term bioassay  
611 experiments, *Biogeosciences*, 11, 3695-3706, 2014.

612 Marie, D., Brussaard, C. P., Thyraug, R., Bratbak, G., and Vaultot, D.: Enumeration of  
613 marine viruses in culture and natural samples by flow cytometry, *Appl Env Microbiol*,  
614 65, 45-52, 1999.

615 Menden-Deuer, S., and Lessard, E. J.: Carbon to volume relationships for dinoflagellates,  
616 diatoms, and other protist plankton, *Limnol Oceanogr*, 45, 569-579, 2000.

617 Mojica, K. D., Huisman, J., Wilhelm, S. W., and Brussaard, C. P.: Latitudinal variation in  
618 virus-induced mortality of phytoplankton across the North Atlantic Ocean, *The ISME*  
619 *journal*, 10, 500-513, 2016.

620 Motegi, C., Tanaka, T., Piontek, J., Brussaard, C., Gattuso, J., and Weinbauer, M.: Effect of  
621 CO<sub>2</sub> enrichment on bacterial metabolism in an Arctic fjord, *Biogeosciences*, 10, 3285-  
622 3296, 2013.

623 Niiranen, S., Yletyinen, J., Tomczak, M. T., Blenckner, T., Hjerne, O., MacKenzie, B. R.,  
624 Müller-Karulis, B., Neumann, T., and Meier, H.: Combined effects of global climate

625 change and regional ecosystem drivers on an exploited marine food web, *Global*  
626 *Change Biol*, 19, 3327-3342, 2013.

627 Olenina, I., Hajdu, S., Edler, L., Andersson, A., Wasmund, N., Busch, S., Göbel, J., Gromisz,  
628 S., Huseby, S., Huttunen, M., Jaanus, A., Kokkonen, P., Ledaine, I., and Niemkiewicz,  
629 E.: Biovolumes and size-classes of phytoplankton in the Baltic Sea, *Balt.Sea Environ.*  
630 *Proc.*, HELCOM, 144 pp., 2006.

631 Paul, A. J., Achterberg, E. P., Bach, L. T., Boxhammer, T., Czerny, J., Haunost, M., Schulz,  
632 K.-G., Stuhr, A., and Riebesell, U.: No observed effect of ocean acidification on  
633 nitrogen biogeochemistry in a summer Baltic Sea plankton community, *Biogeosciences*  
634 13, 3901-3913, doi:10.5194/bg-13-3901-2016, 2016.

635 Paul, A. J., Bach, L. T., Schulz, K.-G., Boxhammer, T., Czerny, J., Achterberg, E. P.,  
636 Hellemann, D., Trense, Y., Nausch, M., Sswat, M., and Riebesell, U.: Effect of elevated  
637 CO<sub>2</sub> on organic matter pools and fluxes in a summer Baltic Sea plankton community  
638 *Biogeosciences*, 12, 6181-6203, doi:10.5194/bg-12-6181-2015, 2015.

639 Piontek, J., Lunau, M., Handel, N., Borchard, C., Wurst, M., and Engel, A.: Acidification  
640 increases microbial polysaccharide degradation in the ocean, *Biogeosciences*, 7, 1615–  
641 1624, 10.5194/bg-7-1615-2010, 2010.

642 Puhe, J., and Ulrich, B.: *Global climate change and human impacts on forest ecosystems:*  
643 *postglacial development, present situation and future trends in Central Europe,*  
644 *Ecological studies – analysis and synthesis*, Springer, Berlin, 476 pp., 2012.

645 Raven, J. A.: Physiology of inorganic C acquisition and implications for resource use  
646 efficiency by marine phytoplankton: relation to increased CO<sub>2</sub> and temperature, *Plant Cell*  
647 *Environ* 14, 779-794, 1991.

648 Reynolds, C. S.: *Ecology of phytoplankton*, Cambridge University Press, Cambridge, 535  
649 pp., 2006.

650 Riebesell, U., Schulz, K. G., Bellerby, R., Botros, M., Fritsche, P., Meyerhöfer, M., Neill, C.,  
651 Nondal, G., Oeschies, A., and Wohlers, J.: Enhanced biological carbon consumption in  
652 a high CO<sub>2</sub> ocean, *Nature*, 450, 545-548, 2007.

653 Riebesell, U., Achterberg, E., Brussaard, C., Engström-Öst, J., Gattuso, J-P., Grossart, H-P.,  
654 Schulz, K. (Eds): *Effects of rising CO<sub>2</sub> on a Baltic Sea plankton community: ecological*  
655 *and biogeochemical impacts. Special issue in Biogeosciences*, 2015.

656 Romero-Kutzner, V., Packard, T., Berdalet, E., Roy, S., Gagné, J., and Gómez, M.:  
657 Respiration quotient variability: bacterial evidence, *Mar Ecol Prog Ser*, 519, 47-59,  
658 2015.

659 Simon, M., and Azam, F.: Protein content and protein synthesis rates of planktonic marine  
660 bacteria, *Mar Ecol Prog Ser*, 51, 201-213, 1989.

661 Singh, S. K., Sundaram, S., and Kishor, K.: *Photosynthetic microorganisms: Mechanism for*  
662 *carbon concentration*, Springer, Berlin, 131 pp., 2014.

663 Smith, F., and Raven, J. A.: Intracellular pH and its regulation, *Ann. Rev. Plant Physiol.*, 30,  
664 289-311, 1979.

665 Sobrino, C., Segovia, M., Neale, P., Mercado, J., García-Gómez, C., Kulk, G., Lorenzo, M.,  
666 Camarena, T., van de Poll, W., Spilling, K., and Ruan, Z.: Effect of CO<sub>2</sub>, nutrients and  
667 light on coastal plankton. IV. Physiological responses, *Aquat Biol*, 22, 77-93, 2014.

668 Spilling, K., Paul, A. J., Virkkala, N., Hastings, T., Lischka, S., Stuhr, A., Bermudez, R.,  
669 Czerny, J., Boxhammer, T., Schulz, K. G., Ludwig, A., and Riebesell, U.: Ocean  
670 acidification decreases plankton respiration: evidence from a mesocosm experiment,  
671 *Biogeosciences Discuss*, in review, 10.5194/bg-2015-608, 2016.

672 Steeman-Nielsen, E.: The use of radioactive carbon for measuring organic production in the  
673 sea, *J. Cons. Int. Explor. Mer.*, 18, 117-140, 1952.

674 Stepanauskas, R., Edling, H., and Tranvik, L. J.: Differential dissolved organic nitrogen  
675 availability and bacterial aminopeptidase activity in limnic and marine waters, *Microb*  
676 *Ecol*, 38, 264-272, 1999.

677 Steward, G. F., Fandino, L. B., Hollibaugh, J. T., Whitley, T. E., and Azam, F.: Microbial  
678 biomass and viral infections of heterotrophic prokaryotes in the sub-surface layer of the  
679 central Arctic Ocean, *Deep Sea Res Pt I*, 54, 1744-1757, 2007.

680 Suttle, C. A.: Marine viruses—major players in the global ecosystem, *Nature Reviews*  
681 *Microbiology*, 5, 801-812, 2007.

682 Tamminen, T., and Andersen, T.: Seasonal phytoplankton nutrient limitation patterns as  
683 revealed by bioassays over Baltic Sea gradients of salinity and eutrophication, *Mar Ecol*  
684 *Prog Ser*, 340, 121-138, 2007.

685 Tanaka, T., Alliouane, S., Bellerby, R., Czerny, J., De Kluijver, A., Riebesell, U., Schulz, K.  
686 G., Silyakova, A., and Gattuso, J.-P.: Effect of increased pCO<sub>2</sub> on the planktonic  
687 metabolic balance during a mesocosm experiment in an Arctic fjord, *Biogeosciences*,  
688 10, 315-325, 2013.

689 Taylor, A. R., Brownlee, C., and Wheeler, G. L.: Proton channels in algae: reasons to be  
690 excited, *Trends Plant Sci*, 17, 675-684, 2012.

691 Teira E., Fernández A., Álvarez-Salgado X. A., García-Martín E. E., Serret P., Sobrino C.:  
692 Response of two marine bacterial isolates to high CO<sub>2</sub> concentration. *Mar Ecol Prog*

693 Ser, 453, 27-36, 2012. Thingstad, T. F., Hagström, Å., and Rassoulzadegan, F.:  
694 Accumulation of degradable DOC in surface waters: Is it caused by a malfunctioning  
695 microbial loop?, *Limnol Oceanogr*, 42, 398-404, 1997.

696 Wanninkhof, R., and Knox, M.: Chemical enhancement of CO<sub>2</sub> exchange in natural waters,  
697 *Limnol Oceanogr*, 41, 689-697, 1996.

698 Waterbury, J. B., Watson, S. W., Valois, F. W., and Franks, D. G.: Biological and ecological  
699 characterization of the marine unicellular cyanobacterium *Synechococcus*, *Can Bull*  
700 *Fish Aquat Sci*, 214, 120, 1986.

701 Weiss, R., and Price, B.: Nitrous oxide solubility in water and seawater, *Mar Chem*, 8, 347-  
702 359, 1980.

703 Veldhuis, M. J., and Kraay, G. W.: Phytoplankton in the subtropical Atlantic Ocean: towards  
704 a better assessment of biomass and composition, *Deep Sea Res Pt I*, 51, 507-530, 2004.

705 Wiebe, P. H.: Functional regression equations for zooplankton displacement volume, wet  
706 weight, dry weight, and carbon: a correction, *Fish. Bull.*, 86, 833-835, 1988.

707 Yamada, N., and Suzumura, M.: Effects of seawater acidification on hydrolytic enzyme  
708 activities, *J Oceanogr*, 66, 233-241, 2010.

709

710

1

2 Table 1. The standing stock of total particulate carbon (TPC<sub>pool</sub>), dissolved organic carbon (DOC<sub>pool</sub>) and dissolved inorganic carbon (DIC<sub>pool</sub>) at the start of  
3 Phase I in mmol C m<sup>-2</sup> ± SE (n = 2). The DOC<sub>pool</sub> was missing some initial measurements and is the average for all mesocosms assuming that the DOC  
4 concentration was similar at the onset of the experiment. The net change in TPC (ΔTPC), DOC (ΔDOC) and DIC (ΔDIC) are average changes in the standing  
5 stocks during Phase I in mmol C m<sup>-2</sup> d<sup>-1</sup> ± SE (n = 2). Flux measurements of atmospheric gas exchange (CO<sub>2flux</sub>) and exported carbon (EXP<sub>TPC</sub>) plus biological  
6 rates: total respiration (TR), bacterial (BP) and net primary production (NPP<sub>14C</sub>) and net community production estimated based on organic carbon  
7 pools (NCP<sub>o</sub>) net primary production, are all average for Phase I in mmol C m<sup>-2</sup> d<sup>-1</sup> ± SE (n = 16). SE for NCP<sub>o</sub> was calculated from the square  
8 root of the sum of variance of the three variables used in Eq 6. The NCP<sub>o</sub> was calculated from the net change in carbon pools plus carbon export,  
9 whereas NPP<sub>14C</sub> was measured carbon fixation using radiolabeled <sup>14</sup>C over a 24 h incubation period *in situ*. TR was measured as O<sub>2</sub> consumption and for  
10 comparison with carbon fixation we used a respiratory quotient (RQ) of 1. A total budget of carbon fluxes for ambient and high CO<sub>2</sub> treatments is presented in  
11 Fig 5.

12

13 **Phase I (t0-t16)**

14 <b>CO<sub>2</sub> treatment (μatmfCO<sub>2</sub>)</b>	<b>365</b>	<b>368</b>	<b>497</b>	<b>821</b>	<b>1007</b>	<b>1231</b>
15 <b>Mesocosm number</b>	<b>M1</b>	<b>M5</b>	<b>M7</b>	<b>M6</b>	<b>M3</b>	<b>M8</b>
16 TPC <sub>pool</sub>	417 ± 38	425 ± 39	472 ± 48	458 ± 38	431 ± 48	446 ± 57
17 DOC <sub>pool</sub>	7172 ± 87	7172 ± 87	7172 ± 87	7172 ± 87	7172 ± 87	7172 ± 87
18 DIC <sub>pool</sub>	25158 ± 9	25182 ± 10	25628 ± 8	26295 ± 22	26637 ± 36	26953 ± 48
19 ΔTPC	-4.6 ± 15	-5.2 ± 13	-8.3 ± 13	-8.2 ± 17	-7.0 ± 13	-6.3 ± 20
20 ΔDOC	15.5 ± 58	18.3 ± 30	18.5 ± 33	25.0 ± 36	18.5 ± 73	18.1 ± 63
21 ΔDIC	5.5 ± 5.2	6.9 ± 9.2	-6.1 ± 11	-24 ± 14	-32 ± 20	-49 ± 42
22 CO <sub>2flux</sub>	4.4 ± 0.2	4.8 ± 0.3	-0.8 ± 0.5	-11 ± 1.0	-17 ± 1.4	-23 ± 2.0
23 EXP <sub>TPC</sub>	6.6 ± 0.10	5.6 ± 0.04	5.4 ± 0.07	6.0 ± 0.07	5.6 ± 0.06	6.0 ± 0.05
24 TR	107 ± 9	82 ± 7	81 ± 6	80 ± 8	75 ± 8	74 ± 8
25 BP	27 ± 8	41 ± 6	43 ± 8	41 ± 4	36 ± 5	46 ± 9
26 NPP <sub>14c</sub>	4.8 ± 0.8	11.4 ± 2.1	14.9 ± 3.6	12.3 ± 2.3	11.3 ± 2.4	14.5 ± 2.7
27 NCP <sub>o</sub>	17.4 ± 33	18.7 ± 20	15.6 ± 30	22.8 ± 28	17.1 ± 25	17.8 ± 28

28

29



1 Table 2. The standing stock of total particulate carbon (TPC<sub>pool</sub>), dissolved organic carbon (DOC<sub>pool</sub>) and dissolved inorganic carbon (DIC<sub>pool</sub>) at the start of  
 2 Phase II in mmol C m<sup>-2</sup> ± SE (n = 2). The net change in TPC (ΔTPC), DOC (ΔDOC) and DIC (ΔDIC) are average changes in the standing stocks during  
 3 Phase II in mmol C m<sup>-2</sup> d<sup>-1</sup> ± SE (n = 2). Flux measurements of atmospheric gas exchange (CO<sub>2flux</sub>) and exported carbon (EXP<sub>TPC</sub>) plus biological rates: total  
 4 respiration (TR), bacterial production (BP), measured (NPP<sub>14c</sub>) and net community production estimated based on organic carbon pools (NCP<sub>o</sub>), are all  
 5 average for Phase II in mmol C m<sup>-2</sup> d<sup>-1</sup> ± SE (n = 14). See Table 1 legend for further details.

6  
 7 **Phase II (t17-t30)**

8 <b>CO<sub>2</sub> treatment (μatm fCO<sub>2</sub>)</b>	<b>365</b>	<b>368</b>	<b>497</b>	<b>821</b>	<b>1007</b>	<b>1231</b>
9 <b>Mesocosm number</b>	<b>M1</b>	<b>M5</b>	<b>M7</b>	<b>M6</b>	<b>M3</b>	<b>M8</b>
10 TPC <sub>pool</sub>	339 ± 14	337 ± 20	331 ± 22	318 ± 9	312 ± 12	339 ± 23
11 DOC <sub>pool</sub>	7435 ± 38	7483 ± 37	7487 ± 43	7597 ± 37	7487 ± 61	7479 ± 37
12 DIC <sub>pool</sub>	25247 ± 34	25269 ± 34	25639 ± 8	26177 ± 25	26413 ± 28	26757 ± 45
13 ΔTPC	-2.4 ± 5	-2.3 ± 8	-1.6 ± 14	0.3 ± 6	2.8 ± 4	3.2 ± 8
14 ΔDOC	-0.6 ± 39	2.4 ± 30	3.6 ± 40	8.4 ± 31	11.3 ± 58	9.1 ± 36
15 ΔDIC	22.4 ± 12	17.6 ± 8.1	-0.4 ± 4.5	-10.5 ± 16	-14.2 ± 10	-23.1 ± 13
16 CO <sub>2flux</sub>	1.7 ± 0.3	1.2 ± 0.3	-2.6 ± 0.3	-10 ± 0.5	-14 ± 0.6	-19 ± 1.0
17 EXP <sub>TPC</sub>	3.3 ± 0.08	2.6 ± 0.06	2.5 ± 0.08	2.6 ± 0.06	2.8 ± 0.07	2.9 ± 0.06
18 TR	140 ± 7	127 ± 5	103 ± 3	103 ± 4	101 ± 5	86 ± 4
19 BP	66 ± 17	57 ± 8	61 ± 7	57 ± 7	43 ± 6	47 ± 6
20 NPP <sub>14c</sub>	3.8 ± 0.6	11.2 ± 1.9	10.8 ± 2.0	14.3 ± 2.8	10.4 ± 2.1	12.0 ± 2.5
21 NCP <sub>o</sub>	0.3 ± 20	2.7 ± 15	4.5 ± 22	11.4 ± 16	16.9 ± 19	15.2 ± 16

22  
 23

1

2 Table 3. The standing stock of total particulate carbon ( $\text{TPC}_{\text{pool}}$ ), dissolved organic carbon ( $\text{DOC}_{\text{pool}}$ ) and dissolved inorganic carbon ( $\text{DIC}_{\text{pool}}$ ) at the start of  
 3 Phase III in  $\text{mmol C m}^{-2} \pm \text{SE}$  ( $n = 2$ ). The net change in TPC ( $\Delta\text{TPC}$ ), DOC ( $\Delta\text{DOC}$ ) and DIC ( $\Delta\text{DIC}$ ) are average changes in the standing stocks during  
 4 Phase III in  $\text{mmol C m}^{-2} \text{d}^{-1} \pm \text{SE}$  ( $n = 2$ ). Flux measurements of atmospheric gas exchange ( $\text{CO}_{2\text{flux}}$ ) and exported carbon ( $\text{EXP}_{\text{TPC}}$ ) plus biological rates: total  
 5 respiration (TR), bacterial production (BP), measured ( $\text{NPP}_{14\text{C}}$ ) and net community production estimated based on organic carbon pools ( $\text{NCP}_o$ ), are all  
 6 average for Phase III in  $\text{mmol C m}^{-2} \text{d}^{-1} \pm \text{SE}$  ( $n = 13$ ). See Table 1 legend for further details. During Phase III we did not have direct measurements of net  
 7 primary production ( $\text{NPP}_{14\text{C}}$ ) or total respiration (TR).

8

9 **Phase III (t31-t43)**

10 <b>CO<sub>2</sub> treatment (<math>\mu\text{atm fCO}_2</math>)</b>	<b>365</b>	<b>368</b>	<b>497</b>	<b>821</b>	<b>1007</b>	<b>1231</b>
11 <b>Mesocosm number</b>	<b>M1</b>	<b>M5</b>	<b>M7</b>	<b>M6</b>	<b>M3</b>	<b>M8</b>
12 $\text{TPC}_{\text{pool}}$	$306 \pm 12$	$304 \pm 20$	$309 \pm 20$	$323 \pm 2$	$351 \pm 13$	$384 \pm 16$
13 $\text{DOC}_{\text{pool}}$	$7426 \pm 16$	$7469 \pm 20$	$7485 \pm 92$	$7553 \pm 20$	$7593 \pm 30$	$7562 \pm 38$
14 $\text{DIC}_{\text{pool}}$	$25557 \pm 9$	$25545 \pm 10$	$25648 \pm 13$	$26030 \pm 19$	$26197 \pm 31$	$26371 \pm 32$
15 $\Delta\text{TPC}$	$-3.8 \pm 10$	$0.3 \pm 7$	$3.3 \pm 14$	$3.3 \pm 10$	$-1.4 \pm 8$	$-4.8 \pm 8$
16 $\Delta\text{DOC}$	$9.8 \pm 5$	$8.8 \pm 7$	$8.9 \pm 43$	$9.2 \pm 10$	$5.7 \pm 17$	$16.3 \pm 20$
17 $\Delta\text{DIC}$	$4.3 \pm 3.9$	$5.5 \pm 8.7$	$6.2 \pm 11$	$-12.3 \pm 7.2$	$-16.3 \pm 14$	$-20.1 \pm 14$
18 $\text{CO}_{2\text{flux}}$	$-0.3 \pm 0.7$	$-0.8 \pm 0.6$	$-3.0 \pm 0.5$	$-7.3 \pm 0.5$	$-9.4 \pm 0.6$	$-13 \pm 0.6$
19 $\text{EXP}_{\text{TPC}}$	$1.5 \pm 0.07$	$1.4 \pm 0.05$	$0.4 \pm 0.07$	$1.9 \pm 0.05$	$1.6 \pm 0.04$	$1.7 \pm 0.05$
20 BP	$31 \pm 6.8$	$37 \pm 1.4$	$38 \pm 1.4$	$27 \pm 2.1$	$17 \pm 3.8$	$28 \pm 2.3$
21 $\text{NCP}_o$	$7.6 \pm 16$	$10.5 \pm 13$	$12.7 \pm 20$	$14.3 \pm 13$	$6.0 \pm 10$	$13.2 \pm 14$

22

23

1

## 2 **Figure legends**

3 Fig. 1. The different fractions of carbon in the control mesocosms (M1 and M5) at the start of  
4 Phase I ( $t_0$ ), II ( $t_{17}$ ) and III ( $t_{31}$ ) in  $\text{mmol C m}^{-2} \pm \text{SE}$  ( $n = 2$ ). The differences between the  
5 controls and elevated  $\text{CO}_2$  concentration are discussed in the text. The size of the boxes  
6 indicates the relative size of the carbon standing stocks.

7 Fig 2. The calculated exchange of  $\text{CO}_2$  between the mesocosms and the atmosphere. Positive  
8 values indicate net influx (ingassing) and negative values net outflux (outgassing) from the  
9 mesocosms. The flux was based on measurements of  $\text{N}_2\text{O}$  as a tracer gas and calculated using  
10 equations 2-5.

11 Fig 3. Change in dissolved inorganic carbon (DIC) pool and the atmospheric  $\text{CO}_2$  exchange  
12 (Fig. 2). All values are average  $\text{mmol C m}^{-2} \text{d}^{-1} \pm \text{SE}$  for the three different phases ( $n = 16$ ,  
13 14 and 13 for Phases I – III respectively) in the control mesocosms (M1 + M5) and high  $\text{CO}_2$   
14 mesocosms (M3 + M8). Black, solid arrows indicated measured fluxes. Grey, dashed arrows  
15 are estimated by closing the budget, and indicate the net community production based on  
16 inorganic carbon budget ( $\text{NCP}_i$ ), which equals biological uptake or release of  $\text{CO}_2$ .

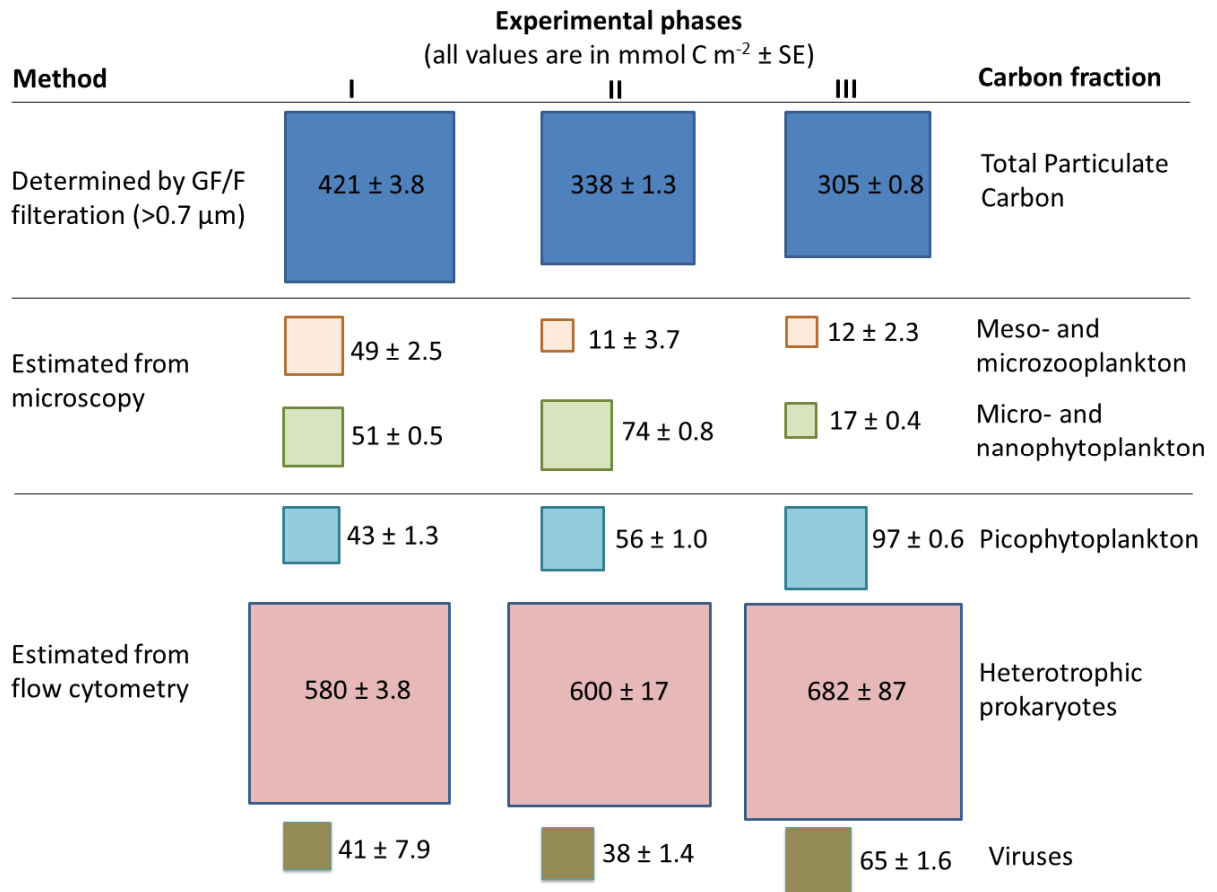
17 Fig 4. Standing stocks of total particulate carbon (TPC) and dissolved carbon (DOC) at the  
18 last day of the experiment ( $t_{43}$ ), plus the sum of exported TPC throughout the experiment; all  
19 values are in  $\text{mmol C m}^{-2} \pm \text{SE}$  ( $n = 2$ ). The values are averages of the two controls (M1 and  
20 M5) and the two highest  $\text{CO}_2$  treatments (M3 and M8). Red circles indicate statistically  
21 significant higher standing stocks in the high  $\text{CO}_2$  treatments (further details in text). The size  
22 of the boxes indicates the relative size of the carbon standing stocks and export.

23 Fig 5. Average carbon standing stocks and flow in the control mesocosms (M1 + M5) and  
24 high  $\text{CO}_2$  mesocosms (M3 + M8) during the three phases of the experiment. All carbon  
25 stocks (squares): dissolved inorganic carbon (DIC), total particulate carbon (TPC) and  
26 dissolved organic carbon (DOC), are average from the start of the period in  $\text{mmol C m}^{-2} \pm \text{SE}$   
27 ( $n = 2$ ). Fluxes (arrows) and net changes ( $\Delta$ ) are averages for the whole phase in  $\text{mmol C m}^{-2}$   
28  $\text{d}^{-1} \pm \text{SE}$  ( $n = 2$ ). Black, solid arrows indicated measured fluxes (Tables 1-3): total respiration  
29 (TR), bacterial production (BP), exported TPC ( $\text{EXP}_{\text{TPC}}$ ). Grey, dashed arrows are estimated  
30 by closing the budget: gross primary production (GPP) using equations 7 and 8; DOC  
31 production ( $\text{DOC}_{\text{prod}}$ ) using equations 9 and 10. Bacterial respiration was calculated using

1 equation 10 and is a share of TR (indicated by the parenthesis). Aggregation was assumed to  
2 equal BP. Red circles indicate statistically higher values compared with the other CO<sub>2</sub>  
3 treatment ( $p < 0.05$ , tests presented in the primary papers described in section 2.2.). The size  
4 of the boxes indicates the relative size of the carbon standing stocks.

5

6

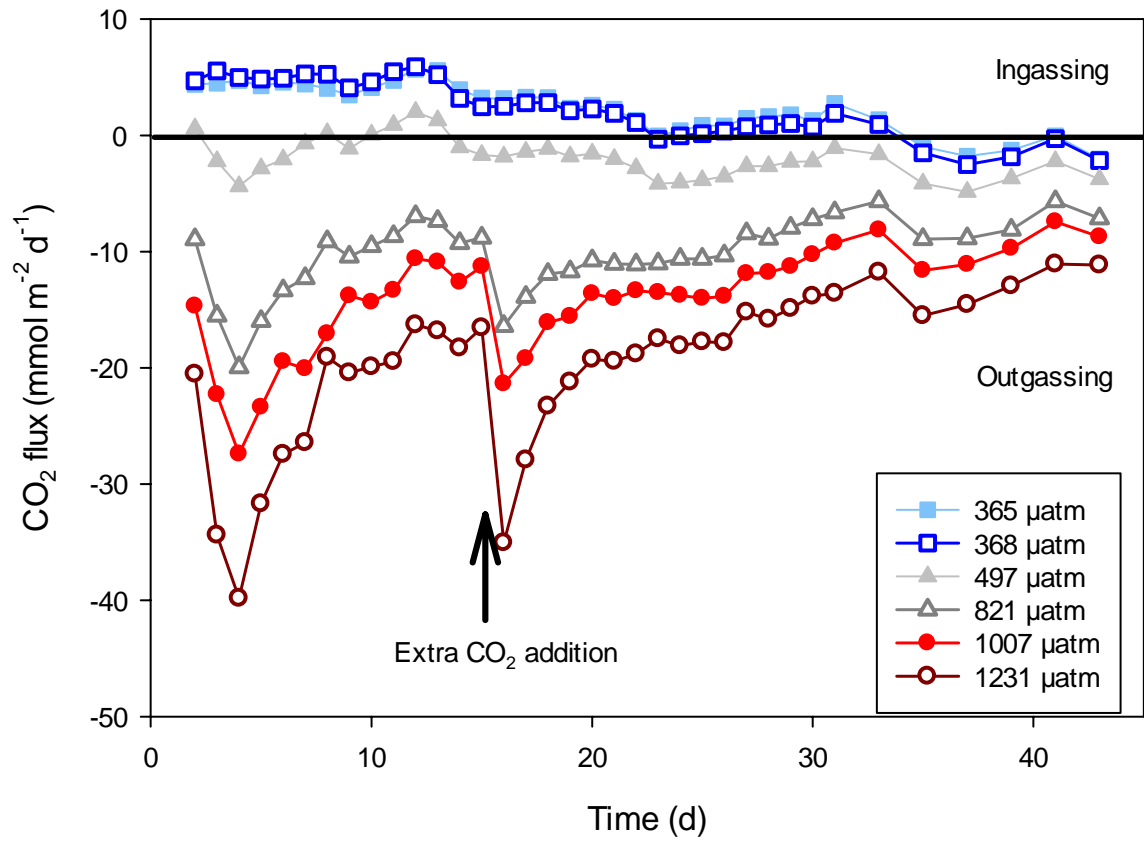


1

2 **Fig 1**

3

4



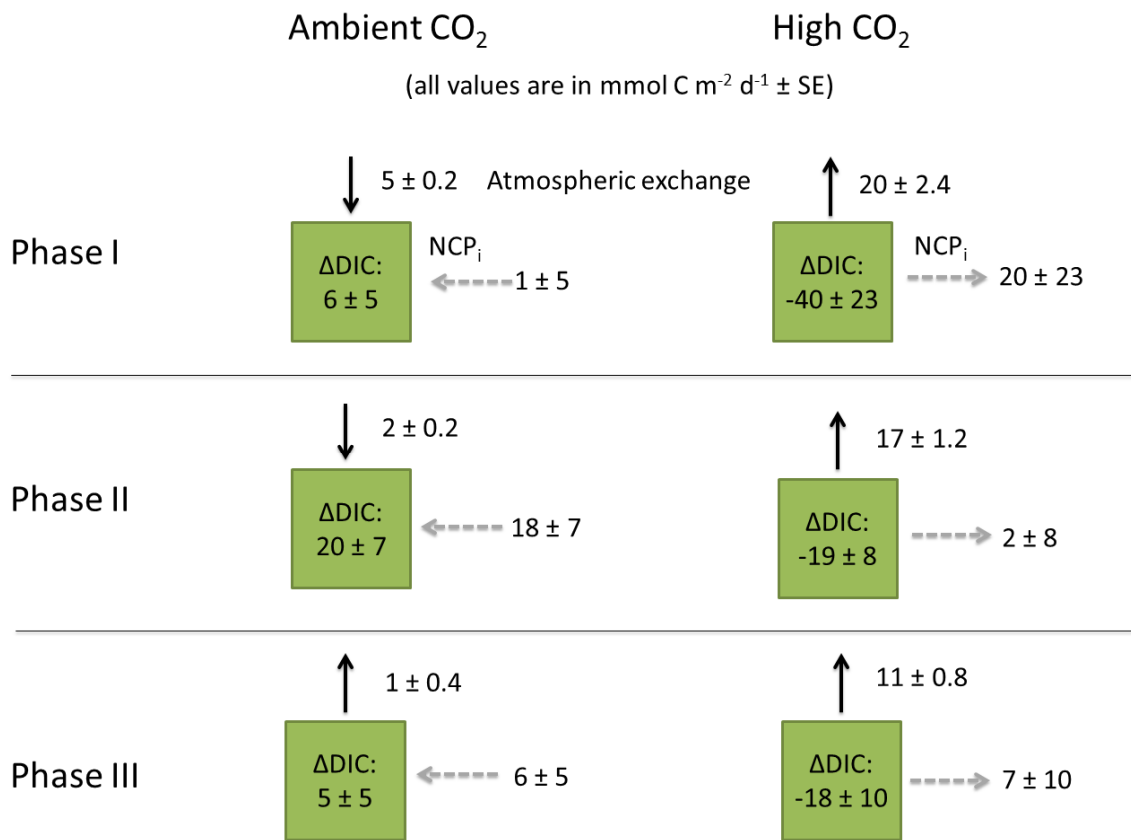
1

2 **Fig 2**

3

4

1  
2



3  
4 **Fig 3**  
5





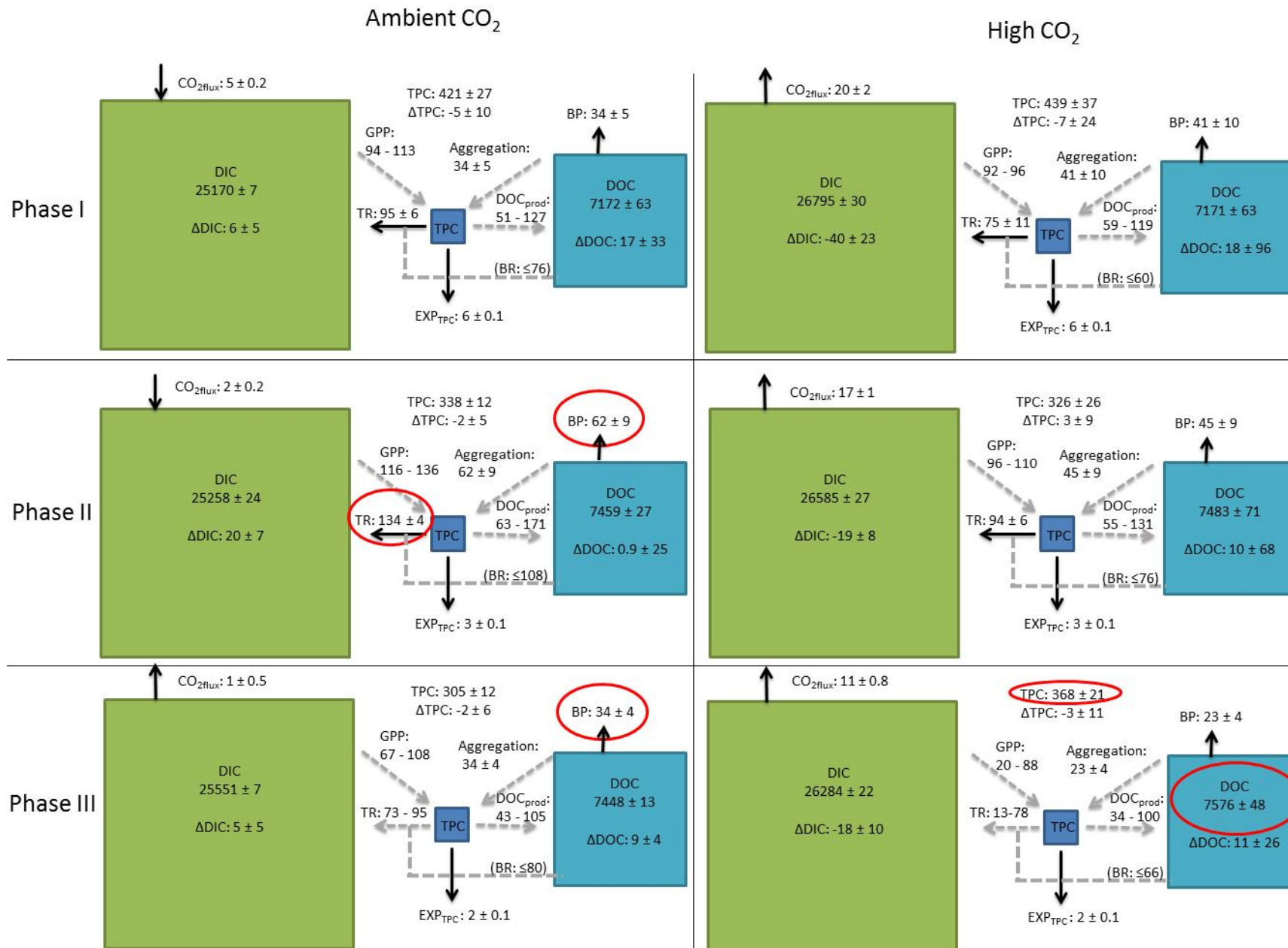


**Fig 5**